BIOLOGY OF REPRODUCTION **85,** 1203–1215 (2011)
Published online before print 10 August 2011
DOI 10.1095/biolreprod.111.093484

Transcriptional Suppression of Sertoli Cell *Timp2* in Rodents Following Mono-(2-ethylhexyl) Phthalate Exposure Is Regulated by CEBPA and MYC[1]

Pei-Li Yao, Yi-Chen Lin, and John H. Richburg[2]

Center for Molecular and Cellular Toxicology, Division of Pharmacology and Toxicology, College of Pharmacy, The University of Texas at Austin, Austin, Texas

ABSTRACT

Our previous studies showed that the prototypical testicular toxic phthalate monoester, mono-(2-ethylhexyl) phthalate (MEHP), suppresses Sertoli cell TIMP2 levels and allows for the activation of MMP2 in seminiferous epithelium. Activation of MMP2 is important for triggering germ cell apoptosis and instigating germ cell detachment from Sertoli cells. These novel findings led us to examine the transcriptional regulation of the *Timp2* gene that accounts for the decrease in Sertoli cell TIMP2 levels following MEHP exposure. Sequential deletion of the *Timp2* 5′-upstream activating sequence (1200 bp) was used to survey transcriptional activation in the *Timp2* promoter region in response to MEHP. Results indicate that under control conditions in rat Sertoli cells, CCAAT enhancer-binding protein alpha (CEBPA) acts as a transactivator to initiate *Timp2* gene transcription, and its action is deactivated by exposure to MEHP. By contrast, MYC protein acts as an inhibitor of *Timp2* gene transcription, and its activity is increased after MEHP treatment. Addition of follicle-stimulating hormone (FSH) to cells causes translocation of CEBPA into the Sertoli cell nucleus and rescues MEHP-suppressed TIMP2 levels. Down-regulation of TIMP2 expression by MEHP exposure is blocked by forskolin (a cAMP-elevating agent), suggesting that the decrease in Sertoli cell TIMP2 expression following MEHP exposure is cAMP-dependent. Taken together, these data indicate that MEHP both disrupts the FSH-stimulated cAMP signaling pathway and activates the inhibitory signaling mediated by MYC protein, to ultimately account for the cellular mechanism underlying the decreased expression of TIMP2 in Sertoli cells.

CEBPA, MEHP, MYC, Sertoli cells, signal transduction, testis, Timp2, *toxicology, transcriptional regulation*

INTRODUCTION

Maintenance of germ cell homeostasis is crucial for functional mature spermatogenesis. The balance between matrix metalloproteinases (MMPs) and tissue inhibitor of metalloproteinases (TIMPs) in the testis appears to be key in controlling the ability of germ cells to respond to changes in the capacity of Sertoli cells to support germ cell development at the peripubertal age [1, 2]. Testicular TIMP2 protein has been shown to be secreted by Sertoli and Leydig cells and is involved in the regulation of germ cell apoptosis, germ cell migration, and tissue restructuring during early testis development [1, 3]. The novel findings of our previous studies revealed that exposure to mono-(2-ethylhexyl) phthalate (MEHP) inhibits the production of TIMP2 by Sertoli cells and consequently allows for the activation of MMP2. MEHP-activated MMP2 further stimulates its processing of tumor necrosis factor-alpha (TNFA) and its specific disruption of junctional complexes in the seminiferous epithelium [1, 2]. However, despite our understanding of the consequences of MEHP-induced activation of MMP2, the mechanism(s) that accounts for the regulation of *Timp2* gene expression in Sertoli cells is not understood. Human *TIMP2* expression in breast cancer cells has been reported to be cooperatively regulated by nuclear transcription factor-Y (NFY) and specificity protein 1 (SP1) for basal and cAMP-inducible transcription activities [4], while *Timp2* regulation in rodents, particularly in rat Sertoli cells, has not been described. Therefore, in this study we aimed to identify the transcription factors that are essential in driving *Timp2* expression in primary rat Sertoli cells and to decipher the influence of MEHP on the regulation of this gene in order to understand the molecular mechanism(s) involved in MEHP toxicity in the testis.

The interaction between follicle-stimulating hormone (FSH) and its receptor on Sertoli cells determines spermatogenic capacity by stimulating Sertoli cell proliferation and supports normal spermatogenesis during early testis development [5]. One of the physiological mechanisms of FSH is to regulate cell adhesion and migration by altering the expression of MMPs and TIMPs. In Sertoli cells, FSH has been shown to stimulate production of MMP2, MT1-MMP, TIMP1, and TIMP2 through activation of the cAMP pathway, resulting in the remodeling of extracellular matrix [6–8]. Interestingly, MEHP strongly decreases FSH-stimulated cAMP accumulation in Sertoli cells [9]. These findings led us to test whether MEHP-disrupted FSH-cAMP signaling plays a role in the changes observed in Sertoli cell TIMP2 levels following toxicant exposure.

In this study, we evaluated the *Timp2* promoter structure in rat Sertoli cells and identified at least two transcription factors which are important for regulating *Timp2* expression. This is the first report to show that inactivation of CCAAT-enhancer-binding protein alpha (CEBPA) and activation of MYC protein cooperatively act to reduce *Timp2* expression in rodents after MEHP exposure. We also demonstrate that impaired FSH signaling is the primary response to MEHP-induced Sertoli cell injury and, consequently, blocks the cAMP pathway, resulting in suppression of TIMP2.

MATERIALS AND METHODS

Animals and MEHP Exposure In Vivo

Peripubertal (21-day-old) male wild-type C57BL/6J mice were purchased from The Jackson Laboratory (Bar Harbor, ME) and allowed to acclimate in the animal facility for 7 days before experiments. The climate of the animal room

[1]Supported in part by National Institute of Environmental Health Sciences, National Institutes of Health, grants ES016591 to J.H.R. and T32 ES07247 to Y.L., and by a Center for Molecular and Cellular Toxicology grant to Y.L.
[2]Correspondence: FAX: 512 471 5002;
e-mail: john.richburg@austin.utexas.edu

Received: 24 May 2011.
First decision: 19 June 2011.
Accepted: 29 July 2011.

eISSN: 1529-7268 http://www.biolreprod.org
ISSN: 0006-3363

was kept at a constant temperature (22°C ± 0.5°C) at 35%–70% humidity, with a 12L:12D photoperiod. Animals were given standard laboratory chow and water ad libitum. All procedures involving animals were performed according to guidelines of the University of Texas at Austin's Institutional Animal Care and Use Committee. Mice (28-day-old) were given a single dose (1 g/kg, in corn oil) of MEHP (TCI America, Portland, OR) by oral gavage, an established model system for eliciting Sertoli cell dysfunction [2]. Control animals received a similar volume of corn oil vehicle. Vehicle- and MEHP-treated animals were killed by CO_2 inhalation, and testes were removed and either immediately frozen in liquid N_2 for protein analysis or fixed in Bouin solution (Polysciences, Inc., Warrington, PA) for histology analysis.

Isolation of Primary Cells

Primary cocultures of rat Sertoli cells and germ cells were isolated from peripubertal (3- to 4-wk-old) Fisher rats (Harlan Laboratories, Houston, TX) according to our previously published methods as a suitable model for testing the paracrine interaction between Sertoli cells and germ cells [1]. Mixed populations of Sertoli cells and germ cells were plated on 35-mm laminin-coated culture dishes at a density of 2×10^6 cells/3 ml of medium containing Dulbecco modified Eagle/F2 medium (Invitrogen Corp., Carlsbad, CA) with epidermal growth factor (1 ng/ml; Sigma, St. Louis, MO), ITS+ Premix solution (insulin, transferrin, selenious acid, bovine serum albumin, and 10 μg/ml linoleic acid; BD Biosciences, San Jose, CA), gentamicin (50 μg/ml; Invitrogen Corp.), and 1% penicillin-streptomycin (Invitrogen Corp.) and then incubated at 34°C. After 48 h, germ cells were lysed by replacing medium with 20 mM Tris-HCl (pH7.4) to obtain primary Sertoli cells for the luciferase activity assay [10].

Chemical Treatment In Vitro

Primary cocultured cells or primary Sertoli cells were treated with 200 μM of MEHP diluted in dimethyl sulfoxide [1, 11]. Primary Sertoli cells were also incubated with 50 ng/ml FSH (Sigma) for various time periods to determine the effect of FSH on TIMP2 production. Varying concentrations of FSH and forskolin (Calbiochem), an activator of adenylate cyclase that results in increased intracellular levels of cAMP [12, 13], were applied to primary rat coculture cells in the presence or absence of MEHP (200 μM) for 12 h.

Semiquantitative RT-PCR

To measure the level of *Timp2* mRNA expression in primary cells, we isolated total RNA from cells or mice testes by using TRIzol reagent (Invitrogen Corp.). First-strand cDNA was prepared using 5 μg of total RNA with Superscript II reverse transcriptase and oligo(dT) primer (all, Invitrogen Corp.). The forward primer used to detect TIMP2 expression levels was F689, 5′-CAA GTT CTT TGC CTG CAT CA-3′; and the reverse primer was R869, 5′-TCC AGG AAG GGA TGT CAA AG-3′. Glyceraldehyde-3-phosphate dehydrogenase (GAPDH) was quantified as an internal control, using the forward primer F968, 5′-GGC ATT GCT CTC AAT GAC AA-3′; and reverse primer R1190, 5′-TGT GAG GGA GAT GCT CAG TG-3′. PCR was performed using 28 cycles at 92°C for 30 sec, then 54°C for 1 min, and 72°C for 30 sec, followed by 72°C for 5 min, with 1 unit of *Taq* DNA polymerase. PCR products were separated on 1.5% agarose gels, and images were captured using a Kodak Gel Logic 100 imaging system (Kodak, Rochester, NY). Densitometry for bands of PCR products was determined using ImageJ software (National Institutes of Health, Bethesda, MD). The relative expression level of each gene was normalized to that of the *Gapdh* value.

Protein Preparation and Western Blot Analysis

Total protein and nuclear extract preparations from cultured cells and mice tissue, as well as Western blot analysis, were performed as described previously [11]. Total cellular proteins and nuclear extracts were examined using primary antibodies against TIMP2 (1:500 dilution; product no. AF971; R&D Systems, Inc., Cambridge, MA), FSH receptor (FSHR; 1:1000 dilution; product no. ab65975; Abcam, Inc., Cambridge, MA), CEBPA (1:1000 dilution; product no. 2295; Cell Signaling Technology, Inc., Beverly, MA), cAMP response element-binding protein (CREB; 1:500 dilution; product no. 9197; Cell Signaling Technology, Inc.), MYC (c-Myc; 1:1000 dilution; product no. 5605; Cell Signaling Technology, Inc.), TATA box binding protein (TBP; 1:1000 dilution; product no. ab63766; Abcam, Inc.), and α-tubulin (1:2000 dilution; product no. 2144; Cell Signaling Technology) coupled with horseradish peroxidase-conjugated secondary antibody (1:5000 dilution; Santa Cruz Biotechnology, Inc.). ECL substrate (Amersham Bioscience, Piscataway, NJ) was used as the detection reagent. Detection of TBP or α-tubulin was used to ensure equal loading of nuclear extracts or total protein. Images of Western blots were captured using the Kodak Gel Logic 100 imaging system. Densitometry for bands on Western blots was determined by ImageJ software. The relative expression level of each protein was normalized by the value of tubulin or TBP in total proteins or nuclear extracts, respectively.

Measurement of Soluble TIMP2 Derived from Primary Coculture Cells

Activity of TIMP2 secreted from primary cocultured cells was determined by reverse zymography and ELISA. After MEHP (200 μM) was added to primary coculture cells, conditioned medium (serum-free) samples were collected at the indicated time points, centrifuged to remove cellular debris, and directly applied to 15% polyacrylamide gels containing 2 mg/ml gelatin (Sigma) and 160 ng/ml purified active gelatinase A (R&D Systems Inc.). After electrophoresis, gels were washed three times for 15 min each with renaturing buffer (2.5% Triton X-100 in 50mM Tris-HCl, pH 7.5) to remove SDS and restore enzyme activity and incubated overnight at 37°C in developing buffer (50 mM Tris-HCl, pH 7.5, 200 mM NaCl, 10 mM $CaCl_2$, and 0.02% sodium azide). Gels were then stained with a solution of 30% methanol-10% acetic acid containing 0.5% (w/v) Coomassie brilliant blue G-250 for 30 min and destained in the same solution without dye. Darkly stained bands against a clear background displayed the presence of TIMPs. In addition, conditioned medium samples collected at various time points were also assayed for soluble TIMP2 by ELISA (R&D Systems, Inc.) following the manufacturer's protocol. Cell numbers were counted to normalize the protein expression assayed by ELISA.

Immunohistochemistry

Expression and localization of TIMP2 in the seminiferous epithelium were determined by immunohistochemistry. Cross-sections (5 μm) of paraffin-embedded testes were deparaffinized and rehydrated, and antigens were unmasked by heating in a 10 mM sodium citrate solution. Sections were incubated with 3% H_2O_2 to block endogenous peroxidase activity and then incubated in blocking buffer containing 10% horse serum. The primary antibody used in this study was goat-anti-TIMP2 (1:100 dilution). Sections were incubated in primary antibody at 4°C overnight. Immunodetection was performed using a VectaStain ABC kit (Vector Labs, Burlingame, CA) and diaminobenzidine substrate (Vector Labs). All sections were captured using a Nikon E800 microscope with a Canon-5D digital camera.

Construction of a Luciferase Reporter Gene

The expression of a luciferase gene under the control of the *Timp2* 5′-upstream activating sequence (5′-UAS; NCBI reference sequence NC_005109.2) was used to evaluate the effects of MEHP exposure on primary rat Sertoli cells. TIMP2-P1200, a 1200-bp region upstream of the *Timp2* promoter (−1 to −1200 bp), was PCR amplified. Five deletion constructs of *Timp2* 5′-UAS were generated by PCR using the TIMP2-P1200 fragment as the template. Predicted transcription factor binding sites were determined from the PROMO website using the TRANSFAC database version 8.3 (http://alggen.lsi.upc.es/cgi-bin/promo_v3/promo/promoinit.cgi?dirDB=TF_8.3). The common reverse primer and distinct forward primers used for each successive fragment are shown in Table 1. Primers were designed to contain overhanging sites for restriction enzymes *Hind*III and *Nhe*I, which allowed for directional cloning into the multiple cloning site of luciferase-expressing vector plasmid pGL-3-enhancer (Promega Corp., Madison, WI). The composition of each construct was confirmed by restriction endonuclease digestion and DNA sequencing.

Transfection and Luciferase Activity Assay

All transfections were carried out in triplicate in 6-well cell culture plates. Primary rat Sertoli cells were transiently transfected using Lipofectamine transfection reagent (Invitrogen Corp.). Luciferase reporter constructs (10 μg) described above or the mock plasmid (pGL3-enhancer vector only) were cotransfected with 1 μg of the beta-galactosidase construct pCMV-beta (Promega Corp.). Cells were incubated in transfection mixture for 6 h and recovered by changing to fresh medium at 18 h. Transfected cells were pretreated with FSH (50 ng/ml) for 6 h to stimulate production of *Timp2* and then treated with MEHP (200 μM) for another 6 h. Cell lysates were prepared in 200 μl of lysis buffer (luciferase assay kit; Roche, Indianapolis, IN). The intensity of luminescence was measured with a Victor3 multilabel reader (PerkinElmer, Waltham, MA). Beta-galactosidase activity was assayed with the same reader using the cell lysates incubated with beta-galactosidase substrate reagents (beta-galactosidase assay kit; Roche). Luciferase activity was normalized by dividing the mean relative luciferase units by the mean relative

TABLE 1. Nucleotide sequence of PCR primers designed to generate sequential deletions in the 5′-UAS of rat *Timp2* gene.

Deletion clone	Primer sequence*
TIMP2-Luc-P1200	F: 5′– CAG CTA GCC TCT CTG TCT CTG TCT –3′
	R: 5′– CCA AGC TTG AGG CGA GGG GAC AGC –3′
TIMP2-Luc-P1000	F: 5′– AAG CTA GCC CAA TTT TTG TCT CTC –3′
	R: 5′– CCA AGC TTG AGG CGA GGG GAC AGC –3′
TIMP2-Luc-P800	F: 5′– CGG CTA GCA GAG CAA AGG TGG CTC –3′
	R: 5′– CCA AGC TTG AGG CGA GGG GAC AGC –3′
TIMP2-Luc-P600	F: 5′– CAG CTA GCT GAC ACT GGC CCC AGA –3′
	R: 5′– CCA AGC TTG AGG CGA GGG GAC AGC –3′
TIMP2-Luc-P400	F: 5′– CGG CTA GCC AGC TGG CCG TTT GGG –3′
	R: 5′– CCA AGC TTG AGG CGA GGG GAC AGC –3′
TIMP2-Luc-P200	F: 5′– CAG CTA GCG AGC GCC CGG CCT GCA –3′
	R: 5′– CCA AGC TTG AGG CGA GGG GAC AGC –3′

* Restriction enzyme cutting sites located within PCR primers are underlined. NheI site, GCTAGC; HindIII site, AAGCTT. F, forward; R, reverse.

beta-galactosidase units. Nontransfected and mock-transfected cells were used as negative controls.

Dpn*I-Mediated Site-Directed Mutagenesis*

To confirm that the identified *cis*-regulatory element is essential for suppressing *Timp2* expression after MEHP exposure, *Dpn*I-mediated site-directed mutagenesis was performed to alter its sequence. *Dpn*I endonuclease targeting sequence 5′-GmATC-3′ is specific for methylated and hemimethylated DNA [14, 15]. The designed sequence-specific primers overlapping with and flanking the transcription factor binding sites (CREB, CEBPA, and MYC) are shown in Table 2. The pGL3-enhancer-TIMP2-P1200 plasmids were used as templates for the PCR for 12 cycles at 95°C for 30 sec, then 55°C for 1 min, and 68°C for 15 min, with 2.5 pfu of DNA polymerase (Stratagene, La Jolla, CA). *Dpn*I (10 units) was applied to PCR products and incubated at 37°C for 1 h. Methylated, nonmutated parental plasmid DNA was digested and fragmented while the nascent PCR fragment was left intact. The nicked plasmid containing the mutation was transformed into *Escherichia coli* to screen for mutant colonies, and the mutation site was verified by DNA sequencing.

Electrophoretic Mobility Shift Assay

Double-stranded oligonucleotides containing CREB, CEBPA, and MYC binding sequences designed for the electrophoretic mobility shift assay (EMSA) are shown in Table 2. The forward and reverse oligonucleotides were annealed to each other to generate double-stranded binding fragments. Nuclear extracts (5 ng) from nontreated or MEHP-treated (6-h) primary rat Sertoli cells were incubated with double-stranded CREB, CEBPA, and MYC binding fragments at room temperature for 20 min by using an EMSA kit (Invitrogen Corp.) [16]. Products of the hybridization reaction were resolved by electrophoresis on 6% nondenaturing polyacrylamide gels at 150V in 0.5× Tris-borate-ethylenediaminetetraacetic acid (EDTA) buffer for 30 min at 4°C. DNA-protein-binding activities were determined by staining gels with SYBR Green EMSA stain (1:10 000) for 20 min at room temperature and then rinsed twice with deionized H_2O. Gels were visualized and analyzed using a FLA-3000 model fluorescent imager (Amersham Bioscience) at wavelength settings of 473 nm excitation and 520/580 nm emission. Densitometry for shifted bands was determined by using ImageJ software. Relative intensity of the shifted band was normalized by the value from the control group.

Chromatin Immunoprecipitation

Chromatin immunoprecipitation (ChIP) assays were performed using a chromatin immunoprecipitation assay kit (Upstate Chemicon, Temecula, CA) according to the manufacturer's instructions. Briefly, primary rat Sertoli cells were cultured in 6-well plates. After cells were treated with 200 μM of MEHP for 6 h, they were cross-linked with 1% formaldehyde and sonicated at an output setting of 30% (Sonic Dismembrator 550; Fisher Scientific, Houston, TX), followed by centrifugation for 15 min at 16 000 × *g* at 4°C. Supernatant (20 μl) was taken as an input control, and the rest of the sample was divided into five portions. Immunoprecipitating antibodies against CREB, CEBPA, MYC, and NFKB1 and 2 μg of normal rabbit immunoglobulin G (IgG; all, Santa Cruz Biotechnology, Inc.) were added to each portion. Cultures incubated with NFKB1 antibody and rabbit IgG served as negative controls. After overnight incubation at 4°C, antibody-histone-DNA complexes were sequentially washed with low-salt buffer, high-salt buffer, LiCl immune buffer, and Tris-EDTA buffer. Precipitates were eluted and incubated at 65°C overnight to reverse formaldehyde cross-linking. DNA was purified by phenol-chloroform extraction and ethanol precipitation. Chromatin fragments were amplified by PCR using primers flanking the specific transcription factor

TABLE 2. The sequences of oligonucleotide designed to generate mutations and perform EMSA based on specific transcription factor binding elements in the 5′-UAS of rat *Timp2* gene.

Clone	Oligonucleotide sequence*
TIMP2-CREB	S: 5′– TAC AGC CCA AGG TGA CCT CAG ACT GAC TCT AGT TCT –3′
	AS: 5′– AGA ACT AGA GTC AGT CTG AGG TCA CCT TGG GCT GTA –3′
TIMP2-ΔCREB	S: 5′– TAC AGC CCA AGG TGA**at**T CAG ACT GAC TCT AGT TCT –3′
	AS: 5′– AGA ACT AGA GTC AGT CTG A**at** TCA CCT TGG GCT GTA –3′
TIMP2-CEBPA	S: 5′– CTC AGT CCC CCA AGT GTT GCC AAA ACG TGT GTG TCC –3′
	AS: 5′– GGA CAC ACA CGT TTT GGC AAC ACT TGG GGG ACT GAG –3′
TIMP2-ΔCEBPA	S: 5′– CTC AGT CCC CCA AGT G**gg c**CC AAA ACG TGT GTG TCC –3′
	AS: 5′– GGA CAC ACA CGT TTT GG**g cc**C ACT TGG GGG ACT GAG –3′
TIMP2-MYC1	S: 5′– GTT TGG GGG AAC CAG AAG TGT GTG GGT GCC ACC CCG –3′
	AS: 5′– CGG GGT GGC ACC CAC ACA CTT CTG GTT CCC CCA AAC –3′
TIMP2-ΔMYC1	S: 5′– GTT TGG GGG AAC CAG AAG **ct**T GTG GGT GCC ACC CCG –3′
	AS: 5′– CGG GGT GGC ACC CAC A**ag** CTT CTG GTT CCC CCA AAC –3′
TIMP2-MYC2	S: 5′– CGG CGC AGC GTG CCA GGT GGT GCG GGA AGC CCG CAG –3′
	AS: 5′– CTG CGG GCT TCC CGC ACC ACC TGG CAC GCT GCG CCG –3′
TIMP2-ΔMYC2	S: 5′– CGG CGC AGC GTG CCA GGT **acc** GCG GGA AGC CCG CAG –3′
	AS: 5′– CTG CGG GCT TCC CGC **ggt** ACC TGG CAC GCT GCG CCG –3′

* The designed sequence flanking the transcription factor binding site are identified by underlines and the mutation sites are identified by boldface lowercase letters. S, sense; AS, antisense.

TABLE 3. Nucleotide sequence of primers designed to perform ChIP assay.

Clone	Primer sequence*	Amplicon
TIMP2-CREB	F: 5′– TGA ATT CAG TAC AGC CCA AGG –3′ R: 5′– TGA CCT GCG AGA CAG AGA GA –3′	−1120 to −970
TIMP2-CEBPA	F: 5′– TGA ATT CAG TAC AGC CCA AGG –3′ R: 5′– TGA CCT GCG AGA CAG AGA GA –3′	−1120 to −970
TIMP2-MYC1	F: 5′– CAG GGA CAA GGC CTG AGT T –3′ R: 5′– GCG CTG TGT ACC TGA TTG C –3′	−448 to −333
TIMP2-MYC2	F: 5′– CCG CAA TCA GGT ACA CAG C –3′ R: 5′– CTC CTC TCG GTG GCT GAC –3′	−353 to −161

* F, forward; R, reverse.

binding sites shown in Table 3, with 50 ng of DNA. PCR consisted of 95°C for 5 min, 30 cycles of 92°C for 1 min, 55°C for 1 min and 72°C for 1 min, and 72°C for 7 min with 1 unit of *Taq* polymerase. PCR products were separated on 1.5% agarose gels, and images were obtained with a Kodak Gel Logic 100 imaging system. Densitometry for bands on PCR products was determined by ImageJ software. The relative expression level of each gene was normalized by the value of the input.

Statistical Analysis

All experiment groups were performed in triplicate and repeated at least three times using different animals and different sets of primary cells. Data were subjected to the Student *t*-test or a parametric ANOVA followed by the Tukey test for post hoc comparisons. Statistical significance was indicated when the P value was <0.05.

RESULTS

Testicular TIMP2 Expression Was Decreased Following MEHP Exposure

Both in vitro and in vivo experimental approaches were performed to evaluate the effect of MEHP challenge on TIMP2 expression levels in the testis. *Timp2* mRNA and protein expression levels were significantly decreased in a time-dependent manner following MEHP exposure in both primary rat Sertoli cell–germ cell cocultures (in vitro) and in C57BL/6J mice testes (in vivo). After 6 h of MEHP exposure, *Timp2* mRNA levels were reduced to 60.1% (in vitro) and 77.4% (in vivo) of control values, respectively (Fig. 1A). In addition, TIMP2 protein levels at 12 h after MEHP exposure were reduced to 62.6% and 85.2% of control values in vitro and in vivo, respectively (Fig. 1B). Measurements of the presence and activity of the soluble form of TIMP2 in the medium from primary cocultures after MEHP exposure, as determined by reverse zymography, showed that the amounts of TIMP2 protein were time-dependently reduced by MEHP treatment (Fig. 1C). A decrease in the amount of soluble TIMP2 was also measured in primary cocultures by ELISA after MEHP exposure (~50% reduction at 12 h) (Fig. 1D). Finally, immunohistochemical staining of testis cross-sections revealed that TIMP2 was localized mainly in Sertoli cells of the seminiferous epithelium and that its expression level was suppressed after MEHP exposure (Fig. 1E).

FSH Treatment Enhanced Production of TIMP2 *mRNA and Protein Levels In Vitro*

In primary rat Sertoli cells, after 6 h of incubation with FSH (50 ng/ml), a significant induction in levels of both TIMP2 mRNA and protein was observed (Fig. 2A). In Figure 2B, primary Sertoli cells transfected with the construct containing the 1200-bp upstream portion of the initiation codon (TIMP2-Luc-P1200) show an approximately 2-fold increase in luciferase activity compared to nontransfected or mock-transfected cells. In control primary rat Sertoli cells, FSH caused a 10-fold induction in luciferase activity, confirming that FSH is able to stimulate *Timp2* transcription in these cells. After MEHP treatment, cells transfected with the P1200 construct showed a smaller amount of luciferase activity than either nontreated or FSH-treated groups. Pretreatment of P1200-transfected cells with FSH followed by MEHP exposure did not result in luciferase activity that was significantly different from that in nontreated cells carrying the P1200 construct. These observations suggested that FSH stimulation of primary rat Sertoli cells is able to trigger induction of *Timp2* transcription and has the ability to rescue transcription activity from MEHP exposure.

Cis-*Regulatory Elements in the −1200 to −1000 bp and −400 to −200 bp Regions of* Timp2 *5′-UAS Are Responsible for MEHP-Induced* Timp2 *mRNA Inhibition*

To identify the regulatory region(s) in the *Timp2* promoter in response to FSH and/or MEHP exposure, we generated a series of fragments based on the 5′-UAS of the *Timp2* promoter (Fig. 3A) and cloned them into a pGL3-enhancer vector to drive luciferase expression. After FSH stimulation, the P1200 construct showed a significant increase in luciferase activity (Fig. 3B), while the P1000 construct had lower activity. The P800, P600, P400, and P200 constructs had levels of luciferase activities similar to that of the P1000 construct following FSH treatment. These observations suggested that the −1200 to −1000 bp region of *Timp2* 5′-UAS may contain important elements for the inducible *Timp2* expression in response to FSH treatment.

MEHP exposure following FSH stimulation revealed significant reduction of luciferase activity in the P1200

FIG. 1. MEHP exposure causes a decrease in testicular TIMP2 levels. In vitro, 2×10^6 primary Sertoli cell–germ cell cocultures were treated with MEHP (200 μM). In vivo, peripubertal male C57BL/6J mice were exposed to MEHP (1 g/kg). **A**) *Timp2* mRNA expression determined by RT-PCR is consistently decreased in vivo and in vitro after MEHP exposure. **B**) Total protein (30 μg) extracted from both cell lysates and whole testis homogenates were analyzed by Western blot analysis. A significant reduction of TIMP2 protein expression is observed following MEHP treatment. Values represent means ± SEM; asterisk indicates significant differences from control (*$P < 0.05$, Student *t*-test). C, control; M, MEHP. The decrease in secretion of soluble TIMP2 in conditioned medium after MEHP exposure was determined by reverse zymography (**C**) and ELISA (**D**). **E**) Testicular cross-sections of MEHP-treated C57BL/6J mice (left, 0 h; right, 12 h) show less expression of TIMP2 (arrowheads) localized in the Sertoli cell cytoplasm than control mice. Bar = 50 μm.

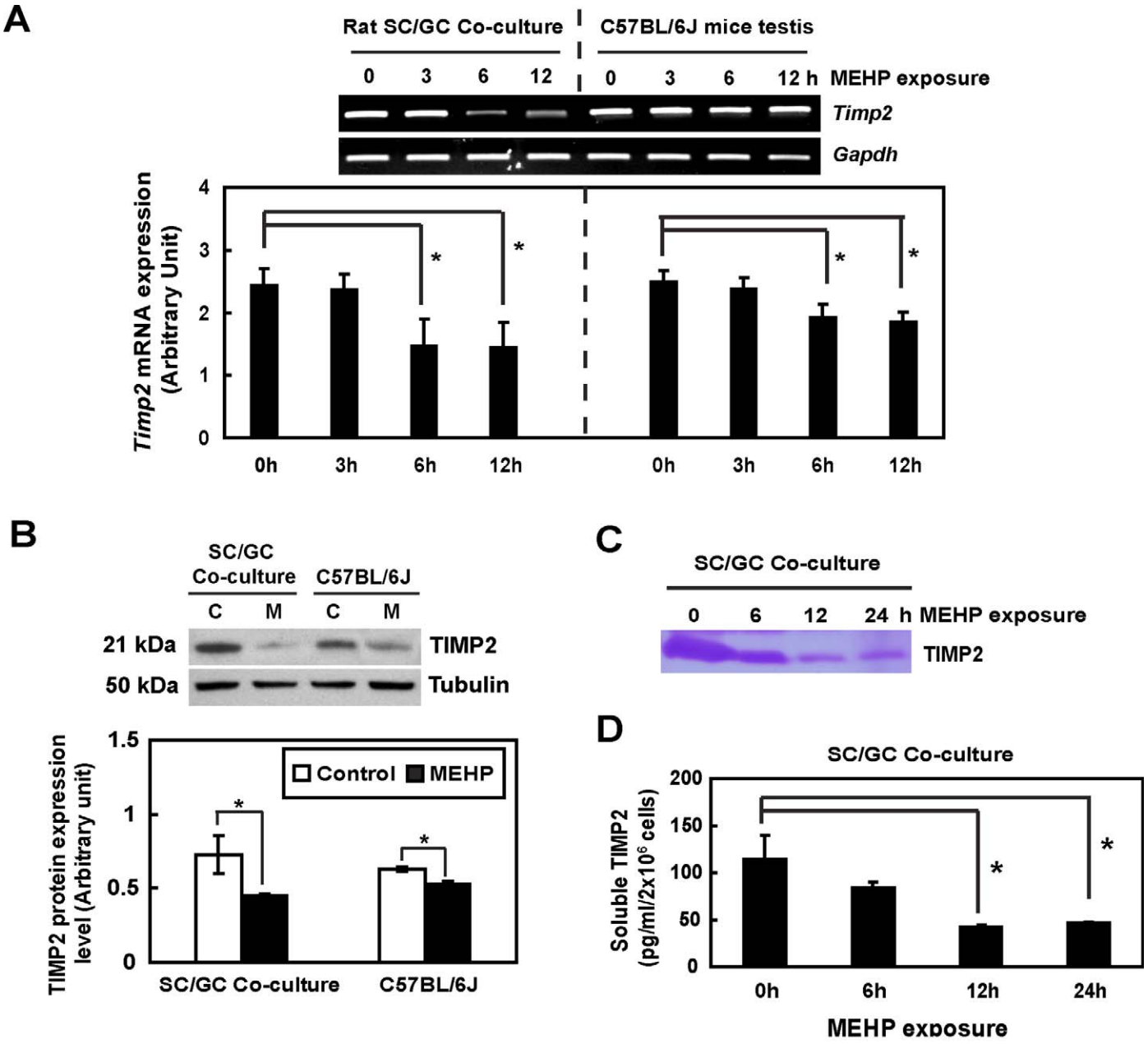

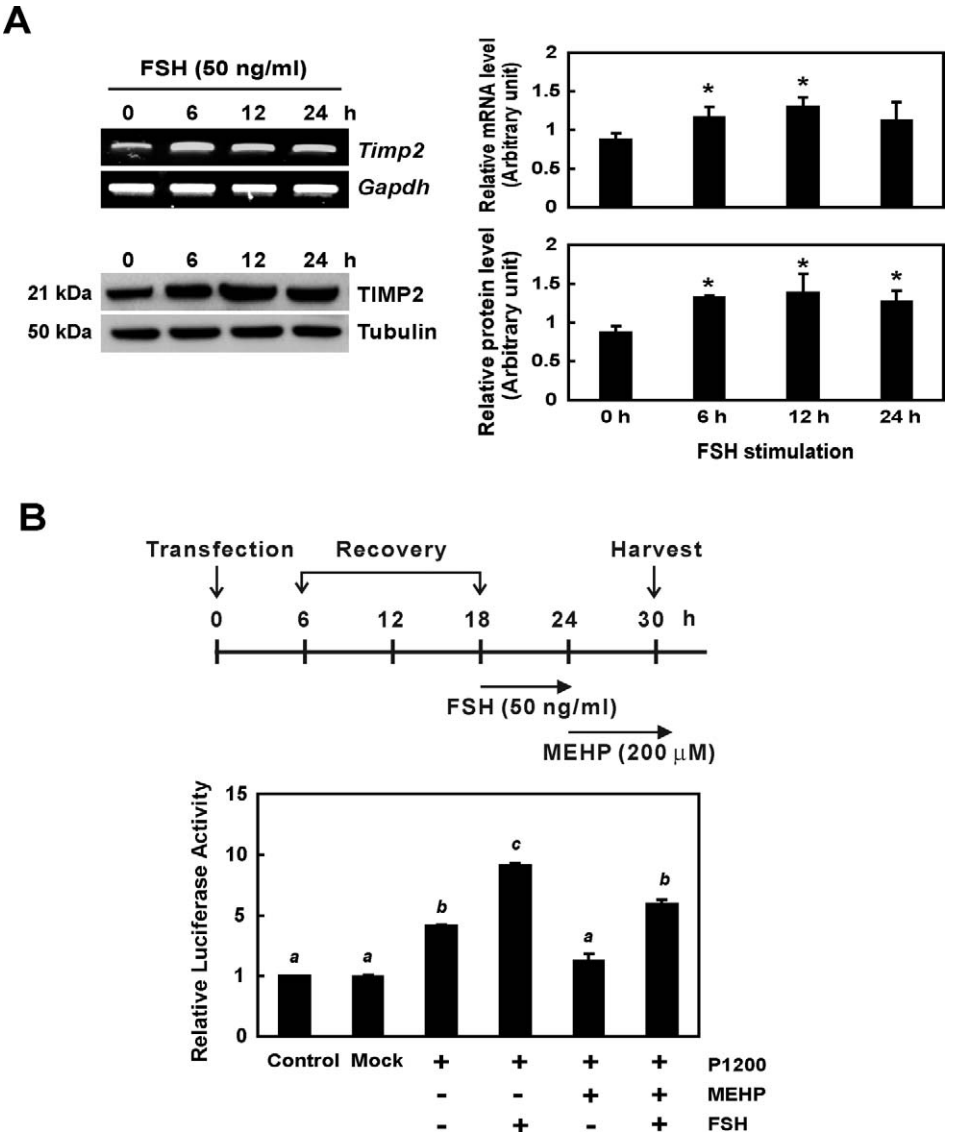

FIG. 2. Effect of FSH on TIMP2 expression in vitro is shown. **A**) Primary rat Sertoli cells were treated with FSH (50 ng/ml) for varying period of time. RT-PCR (upper panel) and Western blot analysis (lower panel) reveal that FSH treatment stimulates both *Timp2* mRNA and protein expression. Values represent means ± SEM, and the asterisk denotes significant difference from control (*$P < 0.05$, Student *t*-test). **B**) A TIMP2-Luc-P1200 (P1200) plasmid carrying a luciferase reporter gene driven by *Timp2* promoter (+1 to −1200 bp) was transfected into primary rat Sertoli cells which were then treated with either MEHP (200 μM) or FSH (50 ng/ml) for 6 h. FSH-MEHP cotreatment was performed by pretreating cells with FSH for 6 h and then adding MEHP for another 6 h. MEHP suppresses luciferase activity of the P1200 construct, while FSH significantly induces its activity, rescuing it from the phenotype seen after MEHP exposure. Significant differences between groups are denoted by bars with different letters (*$P < 0.05$, ANOVA).

construct, while increased luciferase activity was seen in the P200 construct stimulated by FSH alone. No differences were detected among in luciferase activity levels of P1000, P800, P600, and P400 constructs between FSH-treated and FSH-MEHP cotreated groups. These observations suggested that essential *cis*-regulatory element(s) may be located in the −1200 to −1000 bp and −400 to −200 bp regions of the *Timp2* 5′-UAS.

CEBPA and MYC Regulate Timp2 *Expression in Primary Rat Sertoli Cells*

Putative *cis*-regulatory elements in the −1200 to −1000 bp region included binding sites for sex-determining region Y (SRY), heat shock transcription factor-1 (HSF-1), CREB, zinc finger protein 250/647 (ZNF647), and CEBPA. In contrast, activating enhancer-binding protein 4 (AP-4), ZNF647, and MYC are possible inhibitory transcription factors that recognized *cis*-regulatory elements in the −400 to −200 bp region of *Timp2* 5′-UAS with the capacity to suppress *Timp2* expression following MEHP exposure.

To determine whether DNA binding by multiple transcription factors is required for MEHP-decreased *Timp2* expression, four mutant constructs containing mutated CREB, CEBPA, and two MYC binding sequences (TIMP2-Luc-P1200-ΔCREB; ΔCEBPA; ΔMYC1, −380 to −367 bp; and ΔMYC2, −310 to −299 bp) were generated. Transfected primary rat Sertoli cells were pretreated with FSH for 6 h to induce *Timp2* expression. Both the ΔCREB and the ΔCEBPA mutant constructs caused luciferase activities that were lower than those of the wild-type construct after FSH treatment (reduced to 82.3% and 58.6%, respectively, of that of controls), suggesting that CREB and CEBPA are required for FSH-induced *Timp2* expression. The ΔCEBPA mutant construct showed an increase in luciferase activity after MEHP exposure (Fig. 3C). However, the ΔCREB mutant construct still showed significantly reduced luciferase activities after MEHP exposure, indicating that CEBPA and not CREB is a transactivator for controlling *Timp2* expression following MEHP exposure. Both the ΔMYC1 and the ΔMYC2 constructs showed no changes in luciferase activity after FSH treatment compared with the wild-type construct (Fig. 3C), suggesting that MYC is not responsible for FSH-induced *Timp2* expression. The activity of ΔMYC1 was significantly increased following MEHP exposure, while no changes were observed in ΔMYC2 activity (Fig. 3C). Therefore, MYC may serve as an inhibitory transcription factor, binding to the −380 to −367 bp region of the *Timp2* gene.

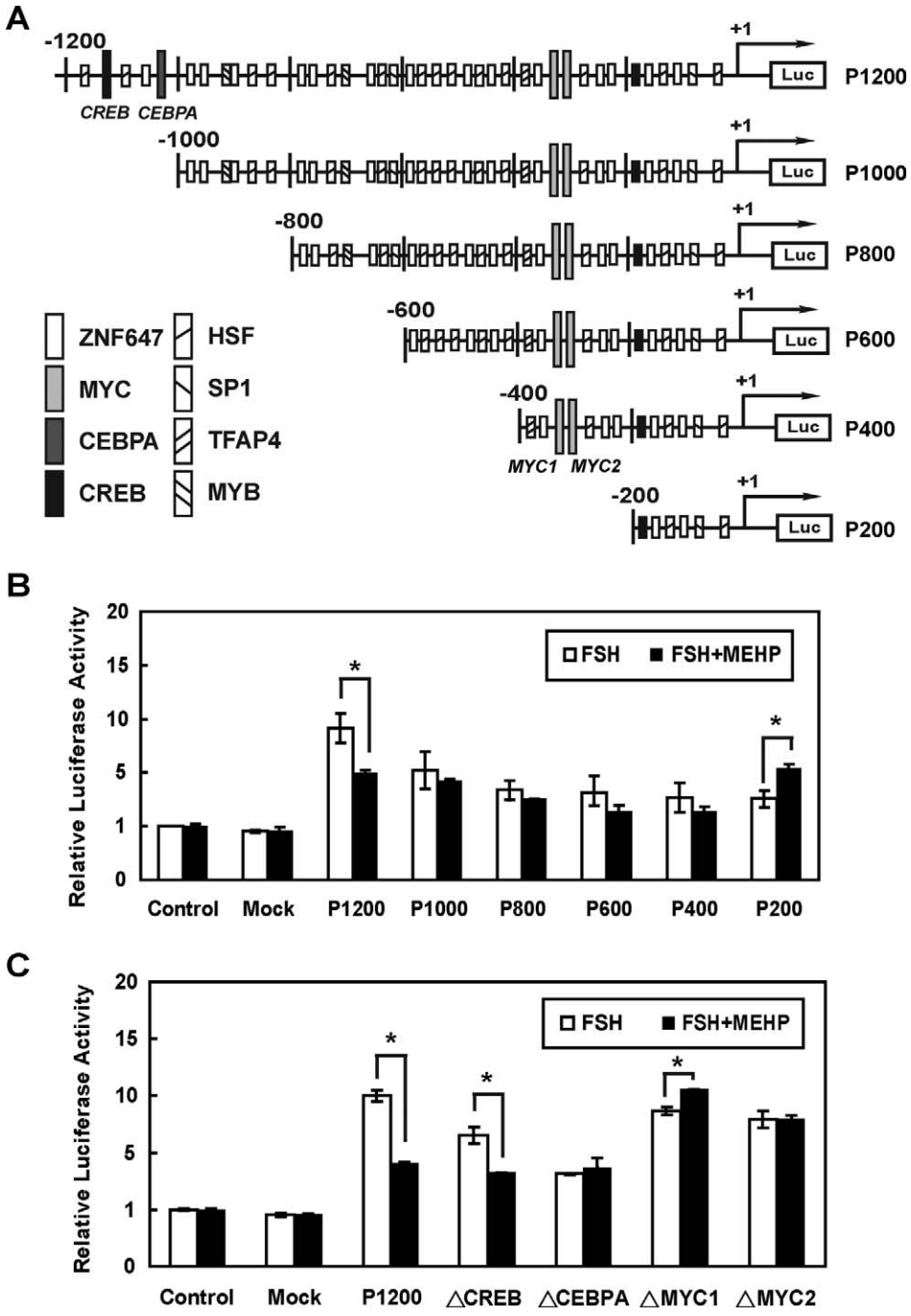

FIG. 3. Functional deletion mapping and the activity of the 5′-UAS of *Timp2* promoter are shown. **A**) Luciferase reporter constructs of *Timp2* 5′-UAS and putative transcription factor binding sites are illustrated. The transcriptional start site in the fragment is indicated by an arrow and +1. Putative transcription binding sites are shown by different boxes. **B**) Luciferase reporter assay was used to measure the activity of the 5′-UAS of *Timp2* promoter. Each construct was transiently cotransfected with pCMV-beta into primary rat Sertoli cells in the presence (solid bars) or absence (open bars) of MEHP following FSH-pretreatment. P1200 showed a significant decrease in luciferase activity after MEHP treatment for 6 h. However, MEHP exposure had no effect on the P1000 construct. P200 shows an increase in luciferase activity in the presence of MEHP. **C**) Site-directed mutagenesis to generate mutant elements (ΔCREB, ΔCEBPA, ΔMYC1, and ΔMYC2) in TIMP2-Luc-P1200 was performed by the *Dpn*I-mediated PCR method. ΔCREB shows a decrease in luciferase activity in the presence of MEHP. ΔMYC1 has a higher activity in MEHP-treated groups. ΔCEBPA and ΔMYC2 show no difference after MEHP treatment. Significant differences between groups are denoted by bars with different letters (*$P < 0.05$, ANOVA).

Next, EMSA and ChIP assays were performed to determine whether endogenous CREB, CEBPA, and MYC are able to bind to these putative binding sites and whether their transcriptional activities are altered after MEHP exposure. Double-stranded DNA fragments encompassing CREB, CEBPA, and two MYC binding sites in the *Timp2* 5′-UAS were incubated with nuclear extracts from primary rat Sertoli cells treated with or without MEHP and resolved on a nondenaturing polyacrylamide gel as described above. Two protein–DNA complexes are formed when nuclear proteins interact with wild-type oligonucleotides. After exposure to MEHP, the intensity of the complex composed of the CREB or CEBPA binding site with higher molecular weight was decreased (0.85- and 0.79-fold, respectively, compared to that of controls) (Fig. 4A), indicating that functional CREB and CEBPA are present in the nuclear extracts of primary rat Sertoli cells and that their DNA-binding activities are suppressed following MEHP exposure. Although MYC in the nuclear extracts of primary rat Sertoli cells was also able to bind to two DNA fragments, binding activity to the MYC1 binding site was increased after MEHP treatment (1.31-fold, compared to that of controls), while no significant changes were observed between control and MEHP-treated MYC2 groups (Fig. 4A). These three proteins all lose their binding activities in the presence of the mutant binding sequences (ΔCREB, ΔCEBPA, ΔMYC1, and ΔMYC2). ChIP assays revealed that anti-CREB, anti-CEBPA, and anti-MYC antibodies were able to pull down cellular DNA fragments containing the *Timp2* promoter, indicating direct interaction between CREB, CEBPA, and MYC and the *Timp2* promoter (Fig. 4B). No significant changes were found in the

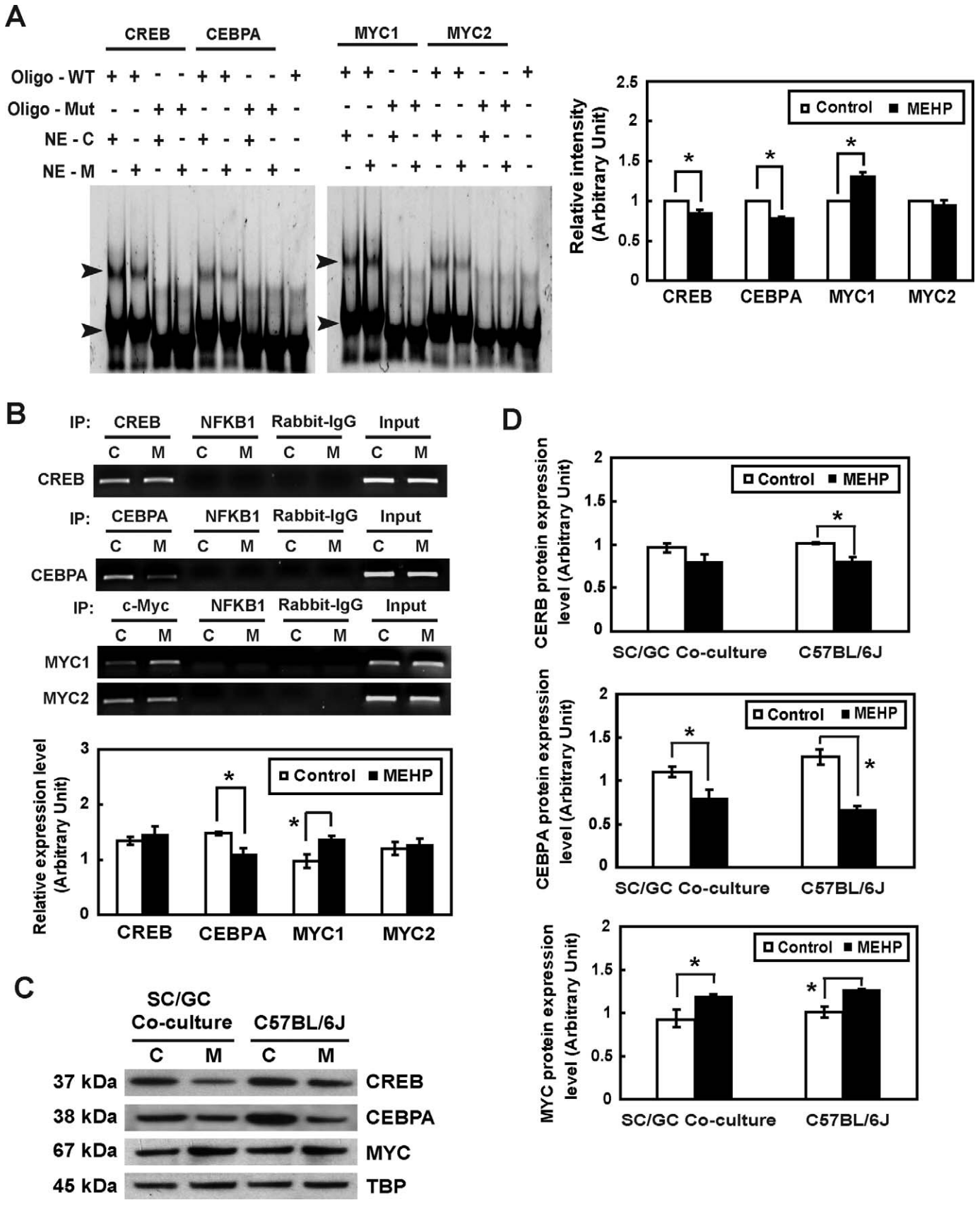

FIG. 4. The influence of MEHP exposure on the transcriptional activity of *Timp2* in vitro is shown. **A**) Detection of CREB, CEBPA, and MYC in Sertoli cells and their interactions with the *Timp2* 5′-UAS in response to MEHP by EMSA are shown. Nuclear extracts (NE) from untreated or MEHP-treated primary rat Sertoli cells were incubated with double-stranded oligonucleotides containing CREB, CEBPA, or MYC binding sequences specific to the *Timp2* 5′-UAS (oligo-WT) or with mutated oligonucleotides (oligo-Mut). The EMSA gel is stained with SYBR Green. The arrowhead indicates the oligonucleotide-protein complex. C, control; M, MEHP. **Right**) Quantitative data of shifted bands with high molecular weight are shown. Values represent means ±

amount of DNA fragments pulled down by anti-CREB antibody after MEHP exposure. The anti-CEBPA antibody pulls down smaller amounts of DNA fragments in the presence of MEHP (0.75-fold, compared to controls), further suggesting that MEHP exposure blocks the ability of CEBPA to bind to *Timp2* promoter. On the other hand, the anti-MYC antibody pulled down larger amounts of DNA fragments containing the −448 to −333 bp region of *Timp2* 5′-UAS (1.38-fold, compared to controls), indicating that the effect MYC had on the regulation of *Timp2* transcription was opposite that of CEBPA (Fig. 4B). Therefore, CEBPA and MYC appear to be relevant and critical regulators of *Timp2* levels in Sertoli cells.

MEHP Exposure Leads to Translocation of MYC but Suppresses CEBPA and CREB

Nuclear protein levels of MYC, CEBPA, and CREB were measured in either primary cocultured cells or whole testis homogenates from C57BL/6J mice (Fig. 4, C and D). The MYC expression level in primary cocultures was 1.58-fold increased at 6 h after MEHP treatment compared to that in the control group. Similar results were observed in vivo, revealing a 1.57-fold increase in MYC expression. CEBPA and CREB expression levels were suppressed in the nucleus following MEHP exposure (in vitro, 0.79- and 0.71-fold; in vivo, 0.83- and 0.69-fold, respectively). These results indicate that MEHP exposure enhances translocation of MYC into the nucleus and inhibits CEBPA and CREB expression.

FSH Signaling Modulates TIMP2 Expression in Primary Rat Sertoli Cell-Germ Cell Cocultures in the Presence of MEHP

The participation of FSH in MEHP-reduced TMP-2 expression was estimated using primary rat cocultured cells. After 12 h of incubation, FSH treatment was able to increase levels of CEBPA and CREB proteins in the nucleus, while MEHP exposure suppressed both nuclear CEBPA and CREB proteins (Fig. 5A). FSH and MEHP cotreatment induced a (1.39-fold) higher level of nuclear CEBPA than that in MEHP-treated cells; however, CREB expression in the nucleus was not rescued by FSH and MEHP cotreatment. FSH stimulation did not affect the expression level of MYC in the Sertoli cell nucleus, while MEHP significantly increased the MYC level (1.38-fold), whether or not FSH was added to the cells. Addition of FSH at any dose in primary rat cocultured cells for 12 h induced the production of TIMP2 without influencing the expression level of FSHR (Fig. 5B). In the presence of MEHP, a low dose (20 ng/ml) of FSH was sufficient to rescue TIMP2 protein expression (~0.94-fold compared to that of nontreated control) (Fig. 5B, right panel). The amount of soluble TIMP2 in primary coculture cells was (1.41-fold) increased by FSH stimulation and (0.68-fold) decreased by MEHP exposure. Cocultured cells with FSH and MEHP cotreatment showed an increase in soluble TIMP2 levels compared to MEHP-treated groups, but those levels were still significantly lower than that of nontreated groups (Fig. 5C). Therefore, the FSH signaling pathway is prominently involved in the regulation of TIMP2 expression following MEHP exposure.

MEHP-Suppressed TIMP2 Expression in Primary Rat Cocultures Is cAMP-Dependent

Because CREB and CEBPA are both well-known downstream effectors in the cAMP signaling pathway, primary rat coculture cells were treated with forskolin, a specific cellular cAMP-elevating agent, to determine whether MEHP-suppressed TIMP2 expression was cAMP-dependent. In the nucleus, levels of CREB and CEBPA expression were strongly increased after forskolin treatment (1.47- and 1.49-fold, respectively, at 10 μM compared to the nontreated group) (Fig. 6A, left panel). CREB and CEBPA expression levels in the nucleus were suppressed in the presence of MEHP but increased by forskolin (1.38- and 1.59-fold, respectively, compared to that in the MEHP-treated group) (Fig. 6A, right panel). Forskolin dose-dependently induced expression of TIMP2 in primary rat cocultured cells (Fig. 6B). MEHP-suppressed TIMP2 expression was also significantly rescued by forskolin at 12 h after treatment (0.99-fold compared to nontreated controls). In addition, forskolin also enhanced (1.52-fold) the amount of TIMP2 secreted in primary cocultured cells and restored production of soluble TIMP2 in response to MEHP (Fig. 6C). These observations indicated that the cAMP signaling pathway plays a key role in driving Sertoli cell TIMP2 expression in response to MEHP.

DISCUSSION

A number of possible mechanisms have been proposed to explain phthalate toxicity observed in the testis, including suppression of FSH-mediated cAMP signaling [9, 17, 18], alterations in the Sertoli cell cytoskeleton [19, 20], and induction of Fas/FasL signaling in the initiation of germ cell apoptosis [21, 22]. We previously demonstrated that MEHP negatively affects distinct junctional complexes between Sertoli cells and germ cells, and consequently, MEHP exposure results in a significant loss of germ cells in the seminiferous tubule [2]. In the testis, TIMP2 is expressed mainly in Sertoli cells and may play a role in cell migration and tissue remodeling during testis development [3, 23, 24]. We previously reported that Sertoli cells reduce their production of TIMP2 in response to MEHP exposure, allowing for activation of MMP2 [1]. The TIMP2:MMP2 ratio appears to be a sensitive and early indicator of MEHP-induced Sertoli cell injury. To understand the primary mechanism of this testicular damage, we further explored the regulation of *Timp2* transcription in the testis following MEHP exposure.

FSH signaling in Sertoli cells supports spermatogenesis, particularly by regulating Sertoli cell proliferation and differentiation [25, 26]. After binding to its receptor on Sertoli cells, FSH stimulates production of intracellular cAMP [27].

SEM with an asterisk denoting significant differences from control (*$P < 0.05$, Student *t*-test). **B**) Binding activities of CREB, CEBPA, and MYC to the *Timp2* 5′-UAS in response to MEHP were determined by ChIP assay. PCR was performed with DNA isolated from primary rat Sertoli cells and then subjected to immunoprecipitation with an anti-CREB, anti-CEBPA, or anti-MYC antibody. Specific primers to the *Timp2* promoter amplified regions containing CREB, CEBPA, MYC1, and MYC2 binding sites. The input represents the amplification of the unprecipitated DNA. PCR amplification of irrelevant immunoprecipitation against anti-NFKB1 antibody and normal rabbit IgG were used as negative controls. Values represent means ± SEM, with the asterisk denoting significant differences from control (*$P < 0.05$, Student *t*-test). **C**) Nuclear extract (30 μg) from primary rat Sertoli cell-germ cell cocultures treated with 200 μM MEHP for 6 h and from C57BL/6J mice testes treated with 1 g/kg of MEHP for 6 h were analyzed by Western blot analysis using antibodies against MYC, CEBPA, and CREB. TBP served as the loading control. **D**) Quantitative data of Western blot analysis are shown. Values represent means ± SEM, with the asterisk denoting significant differences from control (*$P < 0.05$, Student *t*-test).

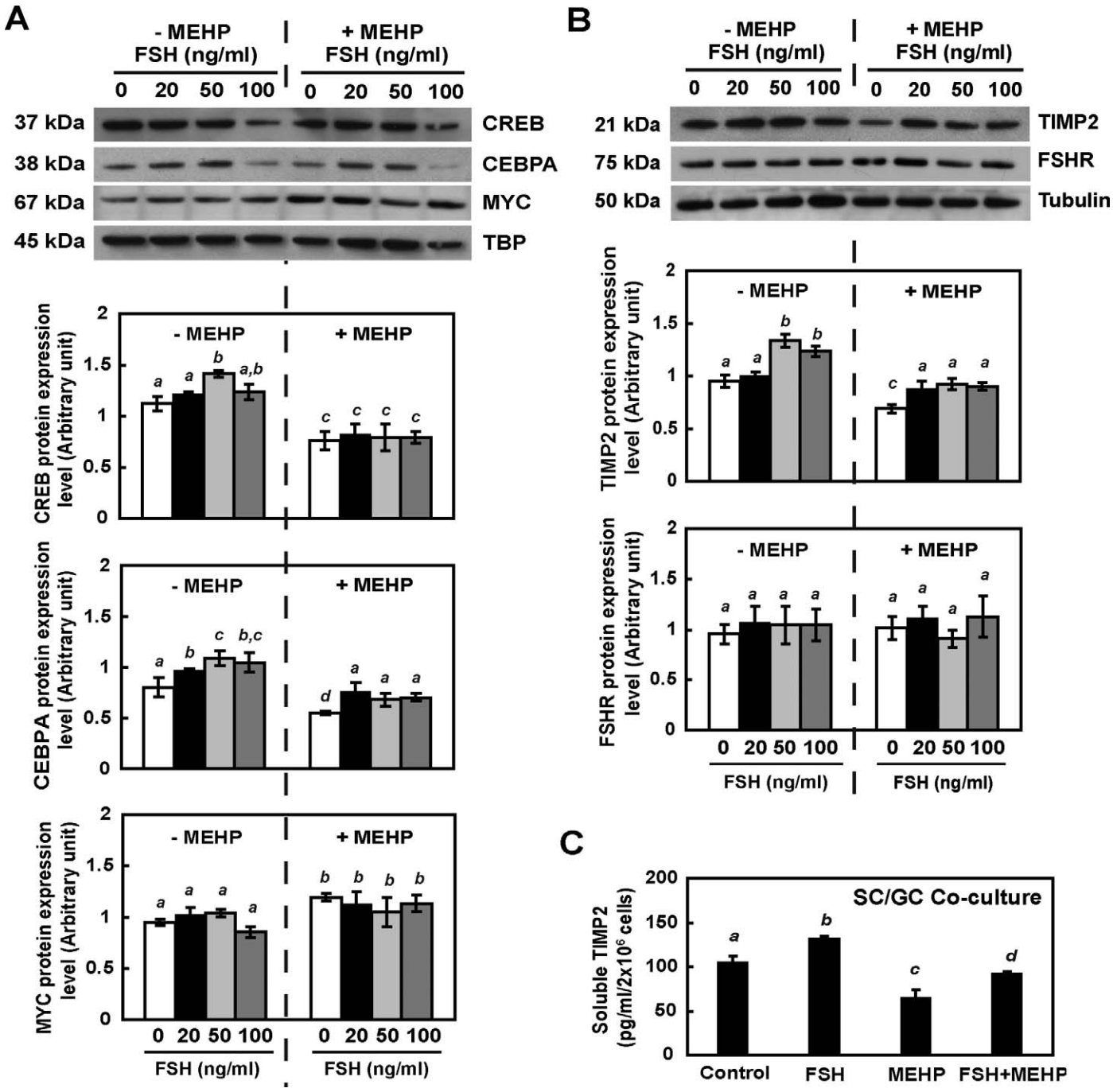

FIG. 5. MEHP-suppressed TIMP2 expression is FSH-dependent in vitro. Nuclear extracts (**A**) and total protein (**B**) from primary Sertoli cell–germ cell cocultures treated with FSH in the absence or presence of MEHP (200 μM) for 12 h were analyzed by Western blot analysis using antibodies against TIMP2, FSHR, MYC, CREB, and CEBPA. Tubulin and TBP serve as loading controls. **C**) The amount of soluble TIMP2 from primary coculture cells following MEHP, FSH (50 ng/ml) treatments, and FSH-MEHP cotreatment was measured by ELISA. Values represent means ± SEM. Significant differences between groups are denoted by bars with different letters (*$P < 0.05$, ANOVA).

This signaling pathway has also been previously shown to be inhibited in the rodent testis after MEHP exposure [9, 18]. Interestingly, TIMP1 and TIMP2 levels are up-regulated by FSH through a cAMP-dependent signaling pathway [7]. These findings led us to hypothesize that MEHP-impaired Sertoli cell FSH-cAMP signaling may be responsible, in part, for the changes observed in Sertoli cell TIMP2 levels.

Several experimental approaches used in the present study, including the *Timp2* promoter sequential deletion strategy, mutation of putative binding sites in the *Timp2* gene, and EMSA and ChIP assays, indicated that CEBPA and MYC played roles in driving *Timp2* expression under hormone and toxicant stimulation conditions. Previous studies have analyzed the structure of the human *TIMP2* promoter, and several transcription factors have been shown to be responsible for regulating its expression. NFY binding to an inverted CCAAT element in the *TIMP2* promoter enhances *TIMP2* levels in 5-azacytidine-treated neuroblastoma cells [28] and is required to activate cAMP-mediated *TIMP2* expression in human breast cancer [4]. In addition, Sp1 may also be important for

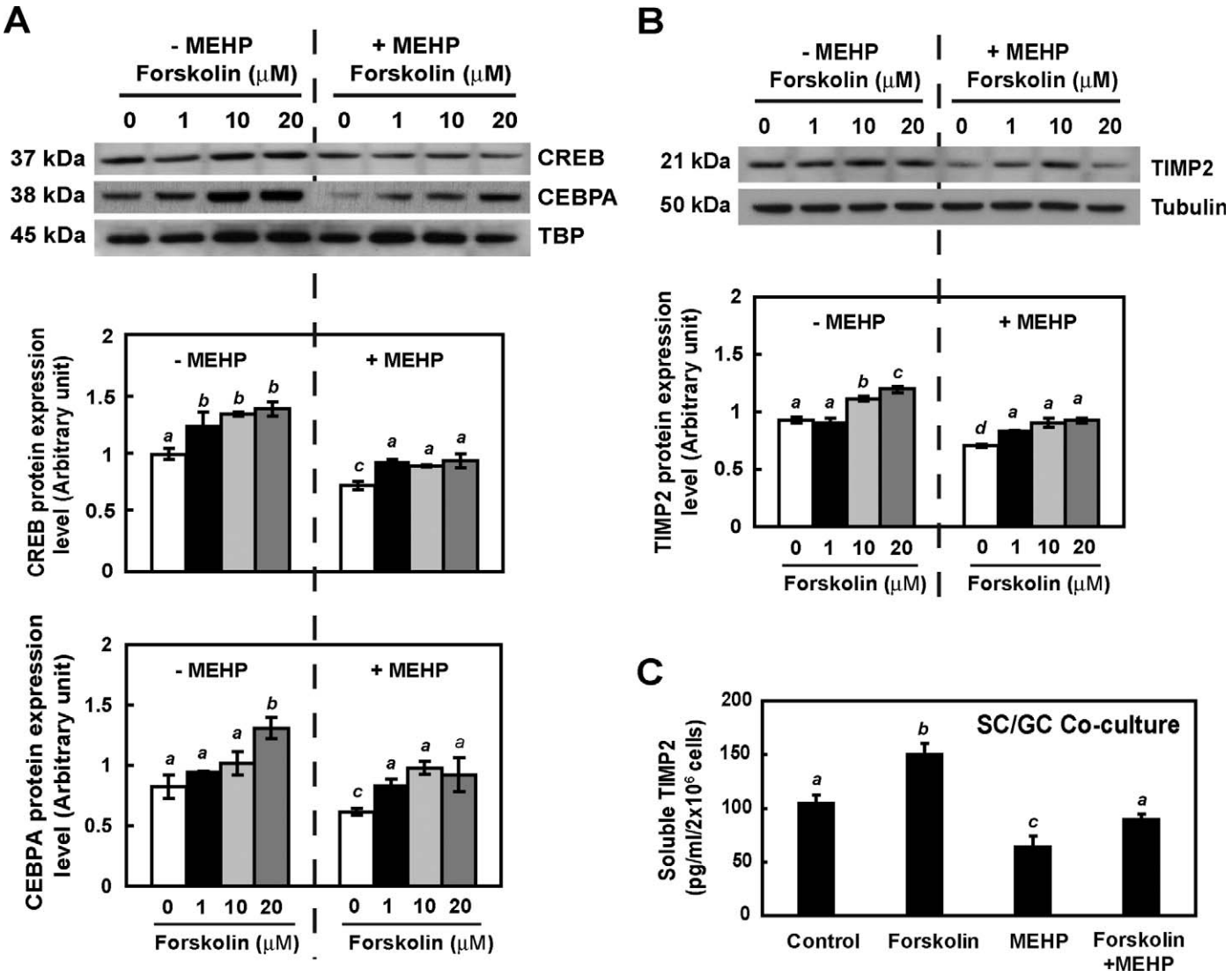

FIG. 6. MEHP-suppressed TIMP2 expression is mediated by cAMP signaling in vitro. Nuclear extracts (**A**) and total protein (**B**) protein from primary Sertoli cell-germ cell cocultures treated with forskolin at various doses in the absence or presence of MEHP (200 μM) for 12 h were analyzed by Western blot analysis using antibodies against TIMP2, CREB, and CEBPA. Tubulin and TBP serve as loading controls. **C**) The amount of soluble TIMP2 from primary coculture cells following MEHP, forskolin (10 μM), and cotreatment was measured by ELISA. Values represent means ± SEM. Significant differences between groups are denoted by bars with different letters (*$P < 0.05$, ANOVA).

regulation of *TIMP2* transcription, depending on the cell type [4, 29]. Interestingly, sequence analysis indicated that there is no NFY binding site (CCAAT-box) present in the rat *Timp2* promoter region. We also found that SP1 is not responsible for either FSH-stimulated or MEHP-suppressed *Timp2* expression (data not shown). A comparison of findings of previous studies using human cells with our observations of rat Sertoli cells suggests that the transcriptional machinery controlling *TIMP2* expression may be species-dependent.

CEBPs are transcription factors modulating cell differentiation and metabolism [30–32]. In the testis, CEBPA, CEBPB, CEBPD, and CEBPZ are present in Sertoli cells [33]. Sertoli cells exposed to chromium(III) chloride have been reported to increase levels of *Cebpa* mRNA, which may influence germ cell development by altering downstream target gene expression [34]. Fetal exposure to dibutyl phthalate (DBP) inhibits steroidogenic genes by decreasing the DNA-binding activity of CEBPB [35]. These studies demonstrated the common participation of the CEBP family after toxicant-induced testicular injury. Our results revealed that after MEHP exposure, both primary rat Sertoli cell-germ cell cocultures and whole testes from C57BL/6J mice show a lower level of CEBPA in the nucleus. We also showed that FSH treatment stimulates the translocation of CEBPA in the Sertoli cell nucleus, even in the presence of MEHP, which may participate in modulating *Timp2* expression. Addition of forskolin significantly rescues CEBPA and TIMP2 expression from MEHP exposure. These data indicate that MEHP-inactivated CEBPA occurs as a consequence of the dysregulation of the FSH-cAMP pathway and consequently a decrease in *Timp2* expression. Although previous studies have already demonstrated the inhibitory effect of MEHP exposure on FSH-cAMP signaling, the present results show compelling, novel evidence linking the MEHP-impaired FSH-cAMP signaling pathway to the down-stream transcriptional dysregulation of *Timp2* in the testis.

The proto-oncogene MYC is a transcription factor responsible for cell proliferation, cell growth, and cell differentiation and acts by both activating and repressing the transcription of down-stream target genes [36]. In this study, we showed that

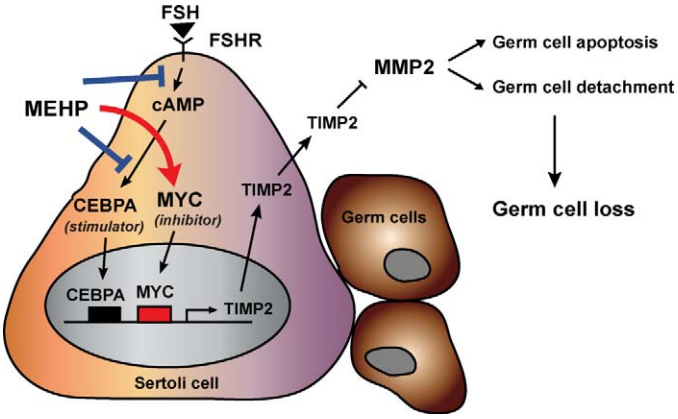

FIG. 7. A refined model shows MEHP-decreased TIMP2 expression in Sertoli cells is mediated by the inactivation of CEBPA and the activation of MYC and is dependent upon the FSH-stimulated cAMP signaling pathway. MEHP exposure causes a decrease in Sertoli cell TIMP2 expression in the seminiferous tubules through transcriptional gene regulation. First, MEHP exposure disturbs cAMP-dependent FSH signaling, leading to the decreased CEBPA observed in the nucleus. Inactivation of CEBPA suppresses TIMP2 levels in Sertoli cells. Second, MEHP exposure activates MYC and contributes to the decrease in TIMP2 expression. MEHP-suppressed TIMP2 allows for activation of MMP2, change in the TIMP2:MMP2 ratio results in stimulating germ cell apoptosis and germ cell detachment.

MEHP exposure causes the activation of MYC in rat Sertoli cells. Similarly, rats exposed to DBP showed an increase in MYC expression level in the liver, and increased MYC expression was associated with DNA repair and synthesis [37]. The molecular mechanism by which MYC interacts with its partner, Max, acting as a transcription activator is well understood [38], while their transcription repression by MYC is not yet fully resolved. By interacting with MIZ1 or SP1, MYC is able to reduce transcriptional activity, leading to a down-regulation of cell cycle-related genes [39–41]. Overexpression of MYCN (N-Myc) causes decreased secretion of TIMP2 in human neuroblastoma cells, allowing for activation of MMP2 and increase in invasive ability [42], indicating that negative regulation of *TIMP2* expression by the MYC family occurs. A microarray study suggested that the function of MYC-repressed genes, including *Timp2*, in rat fibroblasts is related mainly to cell-cell communication and the interaction between cells and their external environment [43]. Our results revealed that deletion or mutation of the MYC binding site on the rat *Timp2* promoter increases transcription activity after MEHP treatment, suggesting that MYC may be a transcription suppressor directly binding to the rat *Timp2* promoter.

In mammals, histone acetylation and DNA methylation play important roles in epigenetic regulation of transcriptional silencing of genes. Hypermethylation of the *TIMP2* promoter causes transcriptional repression of *TIMP2* levels in many types of tumors, including lymphoma and prostate cancer, resulting in tumor metastasis through activation of MMPs [44, 45]. It has been shown that MYC acts as a transcriptional regulator involved in epigenetic modification of its target genes. One possible mechanism that has been proposed is that MYC recruits DNA methyltransferase 3A (DNMT3A), leading to gene silencing by increasing DNA methylation of target promoters [46]. A recent publication demonstrated that the DNMT3-MYC complex promotes methylation of CG sites in cyclin-dependent kinase inhibitor 2A (*CDKN2A*), cyclin D1 (*CCND1*), and *TIMP2* promoters [47]. This leads us to believe that the MYC-mediated transcriptional repression of the *TIMP2* gene described in this study may also involve epigenetic regulation. DEHP-induced testicular toxicity has been recently reported to be involved in DNA hypermethylation in insulin-like hormone 3 (*INSL3*) and mineralocorticoid receptor (*MR*), resulting in a decrease in testosterone production [48, 49]. Therefore, it is necessary to further evaluate the changes in methylation patterns in the testis after MEHP exposure.

We show here that FSH stimulates Sertoli cell TIMP2 expression by activating cAMP-dependent CEBPA and that the overall signaling pathway is disrupted by MEHP exposure, resulting in the decrease in TIMP2 production. However, FSH seems to have no effect on regulating MYC levels in Sertoli cells, based on our results. Only the addition of MEHP in primary cocultured cells causes the activation of MYC. Therefore, MEHP exposure may act as a switch to sensitize Sertoli cells to both deactivate transcription stimulators and activate inhibitors, cooperatively regulating down-stream gene production. According to microarray analysis, many FSH-induced transcripts are identified, including *Crem*, *Cebp,* and *Myc* mRNA in rat Sertoli cells [50]. However, FSH-dependent *Myc* mRNA levels in Sertoli cells have been detected only from 8-day-old animals, not from those at 14–28 days of age [51], suggesting that the effect of FSH on MYC expression may be age-dependent. Primary Sertoli cells isolated from peripubertal rats show that MYC expression is not FSH-mediated, possibly due to difference in age. In addition, MYC has been reported to suppress transcription of *Cebp* and then regulate adipogenesis indirectly [52]. Interactions among FSH, cAMP, C/EBP, and MYC build up a complicated signaling network in the testis in response to MEHP exposure.

Taken together, our present results indicate the direct effect of MEHP on impairing the regulation of *Timp2* transcription through the inactivation of a novel transactivator, CEBPA, together with the activation of a *trans*-acting suppressor, MYC (illustrated diagrammatically in Fig. 7). These findings further revealed the mechanisms in the testis that control expression of TIMP family members. However, as there appears to be distinct differences between human and rat *TIMP2* gene regulation, extrapolation of the MEHP-induced dysregulation of *Timp2* gene expression to mechanisms of human testicular disease after phthalate exposure will require further study.

ACKNOWLEDGMENTS

We thank Jessica Dwyer for expert editorial assistance and Chenan Zhang and Samantha Alexander for performing some of the described experiments.

REFERENCES

1. Yao PL, Lin YC, Richburg JH. TNF alpha-mediated disruption of spermatogenesis in response to sertoli cell injury in rodents is partially regulated by MMP2. Biol Reprod 2009; 80:581–589.
2. Yao PL, Lin YC, Richburg JH. Mono-(2-ethylhexyl) phthalate-induced disruption of junctional complexes in the seminiferous epithelium of the rodent testis is mediated by MMP2. Biol Reprod 2010; 82:516–527.
3. Grima J, Calcagno K, Cheng CY. Purification, cDNA cloning, and developmental changes in the steady-state mRNA level of rat testicular tissue inhibitor of metalloproteases-2 (TIMP-2). J Androl 1996; 17:263–275.
4. Zhong ZD, Hammani K, Bae WS, DeClerck YA. NF-Y and Sp1 cooperate for the transcriptional activation and cAMP response of human tissue inhibitor of metalloproteinases-2. J Biol Chem 2000; 275:18602–18610.
5. Ruwanpura SM, McLachlan RI, Meachem SJ. Hormonal regulation of male germ cell development. J Endocrinol 2010; 205:117–131.
6. Slongo ML, Zampieri M, Onisto M. Expression of matrix metalloproteases (MMP2, MT1 -MMP) and their tissue inhibitor (TIMP-2) by rat sertoli cells in culture: implications for spermatogenesis. Biol Chem 2002; 383:235–239.
7. Ulisse S, Farina AR, Piersanti D, Tiberio A, Cappabianca L, D'Orazi G,

Jannini EA, Malykh O, Stetler-Stevenson WG, D'Armiento M. Follicle-stimulating hormone increases the expression of tissue inhibitors of metalloproteinases TIMP-1 and TIMP-2 and induces TIMP-1 AP-1 site binding complex(es) in prepubertal rat Sertoli cells. Endocrinology 1994; 135:2479–2487.
8. Longin J, Guillaumot P, Chauvin MA, Morera AM, Le Magueresse-Battistoni B. MT1-MMP in rat testicular development and the control of Sertoli cell proMMP2 activation. J Cell Sci 2001; 114:2125–2134.
9. Grasso P, Heindel JJ, Powell CJ, Reichert LE Jr. Effects of mono(2-ethylhexyl) phthalate, a testicular toxicant, on follicle-stimulating hormone binding to membranes from cultured rat Sertoli cells. Biol Reprod 1993; 48:454–459.
10. Galdieri M, Ziparo E, Palombi F, Russo MA, Stefanini M. Pure sertoli cell cultures: a new model for the study of somatic-germ cell interactions. J Androl 1981; 2:249–254.
11. Yao PL, Lin YC, Sawhney P, Richburg JH. Transcriptional regulation of FasL expression and participation of sTNF-alpha in response to sertoli cell injury. J Biol Chem 2007; 282:5420–5431.
12. Scobey MJ, Fix CA, Walker WH. The Id2 transcriptional repressor is induced by follicle-stimulating hormone and cAMP. J Biol Chem 2004; 279:16064–16070.
13. Seamon KB, Padgett W, Daly JW. Forskolin: unique diterpene activator of adenylate cyclase in membranes and in intact cells. Proc Natl Acad Sci U S A 1981; 78:3363–3367.
14. Li S, Wilkinson MF. Site-directed mutagenesis: a two-step method using PCR and DpnI. Biotechniques 1997; 23:588–590.
15. Fisher CL, Pei GK. Modification of a PCR-based site-directed mutagenesis method. Biotechniques 1997; 23:570–571, 574.
16. Jing D, Beechem JM, Patton WF. The utility of a two-color fluorescence electrophoretic mobility shift assay procedure for the analysis of DNA replication complexes. Electrophoresis 2004; 25:2439–2446.
17. Treinen KA, Dodson WC, Heindel JJ. Inhibition of FSH-stimulated cAMP accumulation and progesterone production by mono(2-ethylhexyl) phthalate in rat granulosa cell cultures. Toxicol Appl Pharmacol 1990; 106:334–340.
18. Heindel JJ, Chapin RE. Inhibition of FSH-stimulated cAMP accumulation by mono(2-ethylhexyl) phthalate in primary rat Sertoli cell cultures. Toxicol Appl Pharmacol 1989; 97:377–385.
19. Richburg JH, Boekelheide K. Mono-(2-ethylhexyl) phthalate rapidly alters both Sertoli cell vimentin filaments and germ cell apoptosis in young rat testes. Toxicol Appl Pharmacol 1996; 137:42–50.
20. Kleymenova E, Swanson C, Boekelheide K, Gaido KW. Exposure in utero to di(n-butyl) phthalate alters the vimentin cytoskeleton of fetal rat Sertoli cells and disrupts Sertoli cell-gonocyte contact. Biol Reprod 2005; 73:482–490.
21. Richburg JH, Nanez A. Fas- or FasL-deficient mice display an increased sensitivity to nitrobenzene-induced testicular germ cell apoptosis. Toxicol Lett 2003; 139:1–10.
22. Richburg JH, Nanez A, Gao H. Participation of the Fas-signaling system in the initiation of germ cell apoptosis in young rat testes after exposure to mono-(2-ethylhexyl) phthalate. Toxicol Appl Pharmacol 1999; 160:271–278.
23. Longin J, Le Magueresse-Battistoni B. Evidence that MMP2 and TIMP-2 are at play in the FSH-induced changes in Sertoli cells. Mol Cell Endocrinol 2002; 189:25–35.
24. Siu MK, Cheng CY. Interactions of proteases, protease inhibitors, and the beta1 integrin/laminin gamma3 protein complex in the regulation of ectoplasmic specialization dynamics in the rat testis. Biol Reprod 2004; 70:945–964.
25. Singh J, Handelsman DJ. Neonatal administration of FSH increases Sertoli cell numbers and spermatogenesis in gonadotropin-deficient (hpg) mice. J Endocrinol 1996; 151:37–48.
26. Tarulli GA, Stanton PG, Lerchl A, Meachem SJ. Adult sertoli cells are not terminally differentiated in the Djungarian hamster: effect of FSH on proliferation and junction protein organization. Biol Reprod 2006; 74:798–806.
27. Richards JS. New signaling pathways for hormones and cyclic adenosine 3′,5′-monophosphate action in endocrine cells. Mol Endocrinol 2001; 15:209–218.
28. Cappabianca L, Farina AR, Tacconelli A, Mantovani R, Gulino A, Mackay AR. Reconstitution of TIMP-2 expression in SH-SY5Y neuroblastoma cells by 5-azacytidine is mediated transcriptionally by NF-Y through an inverted CCAAT site. Exp Cell Res 2003; 286:209–218.
29. Lahat N, Bitterman H, Engelmayer-Goren M, Rosenzweig D, Weiss-Cerem L, Rahat MA. Reduced TIMP-2 in hypoxia enhances angiogenesis. Am J Physiol Cell Physiol 2011; 300:C557–C566.
30. Basseres DS, Levantini E, Ji H, Monti S, Elf S, Dayaram T, Fenyus M, Kocher O, Golub T, Wong KK, Halmos B, Tenen DG. Respiratory failure due to differentiation arrest and expansion of alveolar cells following lung-specific loss of the transcription factor C/EBPalpha in mice. Mol Cell Biol 2006; 26:1109–1123.
31. Takeji M, Kawada N, Moriyama T, Nagatoya K, Oseto S, Akira S, Hori M, Imai E, Miwa T. CCAAT/Enhancer-binding protein delta contributes to myofibroblast transdifferentiation and renal disease progression. J Am Soc Nephrol 2004; 15:2383–2390.
32. Koschmieder S, Halmos B, Levantini E, Tenen DG. Dysregulation of the C/EBPalpha differentiation pathway in human cancer. J Clin Oncol 2009; 27:619–628.
33. Gronning LM, Dahle MK, Tasken KA, Enerback S, Hedin L, Tasken K, Knutsen HK. Isoform-specific regulation of the CCAAT/enhancer-binding protein family of transcription factors by 3′,5′-cyclic adenosine monophosphate in Sertoli cells. Endocrinology 1999; 140:835–843.
34. Cheng RY, Alvord WG, Powell D, Kasprzak KS, Anderson LM. Microarray analysis of altered gene expression in the TM4 Sertoli-like cell line exposed to chromium(III) chloride. Reprod Toxicol 2002; 16:223–236.
35. Kuhl AJ, Ross SM, Gaido KW. CCAAT/enhancer binding protein beta, but not steroidogenic factor-1, modulates the phthalate-induced dysregulation of rat fetal testicular steroidogenesis. Endocrinology 2007; 148:5851–5864.
36. Pelengaris S, Khan M. The many faces of c-MYC. Arch Biochem Biophys 2003; 416:129–136.
37. Kostka G, Urbanek-Olejnik K, Wiadrowska B. Di-butyl phthalate-induced hypomethylation of the c-myc gene in rat liver. Toxicol Ind Health 2010; 26:407–416.
38. Luscher B. Function and regulation of the transcription factors of the Myc/Max/Mad network. Gene 2001; 277:1–14.
39. van Riggelen J, Muller J, Otto T, Beuger V, Yetil A, Choi PS, Kosan C, Moroy T, Felsher DW, Eilers M. The interaction between Myc and Miz1 is required to antagonize TGFbeta-dependent autocrine signaling during lymphoma formation and maintenance. Genes Dev 2010; 24:1281–1294.
40. Gartel AL, Ye X, Goufman E, Shianov P, Hay N, Najmabadi F, Tyner AL. Myc represses the p21(WAF1/CIP1) promoter and interacts with Sp1/Sp3. Proc Natl Acad Sci U S A 2001; 98:4510–4515.
41. Staller P, Peukert K, Kiermaier A, Seoane J, Lukas J, Karsunky H, Moroy T, Bartek J, Massague J, Hanel F, Eilers M. Repression of p15INK4b expression by Myc through association with Miz-1. Nat Cell Biol 2001; 3:392–399.
42. Noujaim D, van Golen CM, van Golen KL, Grauman A, Feldman EL. N-Myc and Bcl-2 coexpression induces MMP2 secretion and activation in human neuroblastoma cells. Oncogene 2002; 21:4549–4557.
43. O'Connell BC, Cheung AF, Simkevich CP, Tam W, Ren X, Mateyak MK, Sedivy JM. A large scale genetic analysis of c-Myc-regulated gene expression patterns. J Biol Chem 2003; 278:12563–12573.
44. Pulukuri SM, Patibandla S, Patel J, Estes N, Rao JS. Epigenetic inactivation of the tissue inhibitor of metalloproteinase-2 (TIMP-2) gene in human prostate tumors. Oncogene 2007; 26:5229–5237.
45. Galm O, Suzuki H, Akiyama Y, Esteller M, Brock MV, Osieka R, Baylin SB, Herman JG. Inactivation of the tissue inhibitor of metalloproteinases-2 gene by promoter hypermethylation in lymphoid malignancies. Oncogene 2005; 24:4799–4805.
46. Brenner C, Deplus R, Didelot C, Loriot A, Vire E, De Smet C, Gutierrez A, Danovi D, Bernard D, Boon T, Pelicci PG, Amati B, et al. Myc represses transcription through recruitment of DNA methyltransferase corepressor. Embo J 2005; 24:336–346.
47. Hervouet E, Vallette FM, Cartron PF. Dnmt3/transcription factor interactions as crucial players in targeted DNA methylation. Epigenetics 2009; 4:487–499.
48. Wu S, Zhu J, Li Y, Lin T, Gan L, Yuan X, Xu M, Wei G. Dynamic effect of di-2-(ethylhexyl) phthalate on testicular toxicity: epigenetic changes and their impact on gene expression. Int J Toxicol 2010; 29:193–200.
49. Martinez-Arguelles DB, Culty M, Zirkin BR, Papadopoulos V. In utero exposure to di-(2-ethylhexyl) phthalate decreases mineralocorticoid receptor expression in the adult testis. Endocrinology 2009; 150:5575–5585.
50. McLean DJ, Friel PJ, Pouchnik D, Griswold MD. Oligonucleotide microarray analysis of gene expression in follicle-stimulating hormone-treated rat Sertoli cells. Mol Endocrinol 2002; 16:2780–2792.
51. Lim K, Hwang BD. Follicle-stimulating hormone transiently induces expression of protooncogene c-myc in primary Sertoli cell cultures of early pubertal and prepubertal rat. Mol Cell Endocrinol 1995; 111:51–56.
52. Freytag SO, Geddes TJ. Reciprocal regulation of adipogenesis by Myc and C/EBP alpha. Science 1992; 256:379–382.